

# Preparation and Characterization of Nano structured Materials from Fly Ash: A Waste from Thermal Power Stations, by High Energy Ball Milling

K. Thomas Paul · S. K. Satpathy · I. Manna ·  
K. K. Chakraborty · G. B. Nando

Received: 27 April 2007 / Accepted: 15 June 2007 / Published online: 11 July 2007  
© to the authors 2007

**Abstract** The Class F fly ash has been subjected to high energy ball milling and has been converted into nano-structured material. The nano structured fly ash has been characterized for its particle size by using particle size analyzer, specific surface area with the help of BET surface area apparatus, structure by X-ray diffraction studies and FTIR, SEM and TEM have been used to study particle aggregation and shape of the particles. On ball milling, the particle size got reduced from 60  $\mu\text{m}$  to 148 nm by 405 times and the surface area increased from 0.249  $\text{m}^2/\text{gm}$  to 25.53  $\text{m}^2/\text{gm}$  i.e. by more than 100%. Measurement of surface free energy as well as work of adhesion found that it increased with increased duration of ball milling. The crystallite was reduced from 36.22 nm to 23.01 nm for quartz and from 33.72 nm to 16.38 nm for mullite during ball milling to 60 h. % crystallinity reduced from 35% to 16% during 60 h of ball milling because of destruction of quartz and hematite crystals and the nano structured fly ash is found to be more amorphous. Surface of the nano structured fly ash has become more active as is evident from the FTIR studies. Morphological studies revealed that the surface of the nano structured fly ash is more uneven and rough and shape is irregular, as compared to fresh fly ash which are mostly spherical in shape.

**Keywords** High energy ball mill · Fly ash · Nanostructured materials · Quartz · Mullite

## Introduction

Nanoscience and nanotechnology has become the buzzword in recent years since its inception in 1990's. It literally means any technology performed in the nanoscale down to molecular level. Nanotechnology encompasses the production and application of physical, chemical and biological systems at scales ranging from individual atoms or molecules to submicron level as well as integration of the resulting nano structure to larger systems [1]. Nanomaterial is defined as the materials with the microstructure having at least one dimension in nanometer range. It has appeal of miniaturization; also it imparts enhanced electronic, magnetic, optical and chemical properties to a level that cannot be achieved by conventional materials. The key characteristics of nanomaterials are its small size, narrow size distribution, low levels of agglomeration and high dispersability [2].

A variety of ways have been reported to synthesize nano level materials such as plasma arcing, chemical vapor deposition, electro deposition, sol-gel synthesis, high intensity ball milling etc [3]. Among these methods high energy milling has advantages of being simple, relatively inexpensive to produce, applicable to any class of materials and can be easily scaled up to large quantities [4]. In this mechanical treatment, powder particles are subjected to a severe plastic deformation due to the repetitive compressive loads arising from the impacts between the balls and the powder. The high concentration of defects and the continuous interfaces renewal, associated with the milling-induced enhanced atomic mobility, promote different

---

K. T. Paul · S. K. Satpathy · K. K. Chakraborty ·  
G. B. Nando (✉)  
Rubber Technology Centre, Indian Institute of Technology,  
Kharagpur, West Bengal 721302, India  
e-mail: golokb@rtc.iitkgp.ernet.in

I. Manna  
Metallurgical and Materials Engineering Department,  
Indian Institute of Technology, Kharagpur,  
West Bengal 721302, India

phenomena depending on the materials being milled [5–7]. This produces novel crystalline and amorphous materials with crystallite sizes at the nanometer scale.

Coal-burning power plants that consume pulverized solid fuels produce large amounts of fly ash. These are the finely divided mineral residue resulting from the combustion of ground or powdered coal in electric power generating plant. The fly ash consists of inorganic, incombustible matter present in the coal that has been fused during combustion into a glassy, amorphous structure. This material is solidified while suspended in the exhaust gases and is collected by particulate emission control devices, such as electrostatic precipitators or filter fabric bag houses. Fly ash, often called pulverized fuel ash, is the largest produced industrial waste in the world, mainly due to the global reliance on the coal-fired power plants [8]. Since the particles solidify while suspended in the exhaust gases, fly ash particles are mostly spherical in shape and range in size from 0.5  $\mu\text{m}$  to 100  $\mu\text{m}$ . They consist mostly of mullite ( $3\text{Al}_2\text{O}_3 \cdot 2\text{SiO}_2$ ), quartz ( $\text{SiO}_2$ ), aluminium oxide ( $\text{Al}_2\text{O}_3$ ), hematite ( $\text{Fe}_2\text{O}_3$ ), lime ( $\text{CaO}$ ) and gypsum ( $\text{CaSO}_4 \cdot 2\text{H}_2\text{O}$ ). As a result it possesses various physical, chemical and mineralogical properties, depending on the mineralogical composition of the used coal and on the combustion technology [9].

About 75% of India's energy supply is coal based and shall be so for the next few decades. There are about 82 utility thermal power stations to produce approximately 110 million tonnes of fly ash per annum in the Country [10]. Nearly 38% of the fly ash waste is utilized in the Country at present [11], in various fields including landfills, cement making and concrete product making such as bricks, blocks and tiles, in road making, in filling of the mines. Attempts have been made earlier to utilize this fly ash waste in the polymer industry in making polymeric composites where fly ash is being used as inorganic particulate filler without much breakthrough. The utilization of fly ash is determined by their properties such as fineness, specific surface area, particle shape, hardness, freeze-thaw resistance, etc. Many investigations have been carried out towards the effective utilization of fly ash and with understanding of potential environmental and health impacts associated with its disposal by land filling.

In this paper an attempt has been made to modify the fly ash by transforming the micro sized fly ash into nanostructured fly ash using high energy ball mill. The smooth, glassy and inert surface of the fly ash can be altered to a rough and more reactive by this technique. The nano structured fly ash thus obtained may be characterized using sophisticated analytical techniques. Thus, nano level mineral filler can be used as reinforcing filler in making polymer composites, in particular rubber based composites.

## Experimental

### Materials

Fly ash samples collected from Kolaghat Thermal Power Station, West Bengal, India having a specific gravity of 2.33 gm/cc and total evaporable moisture content of 1.54% is used. The particle size of fly ash falls in the range of 60–100  $\mu\text{m}$ . Loss on ignition, which was measured by burning the sample in muffle furnace at 800  $^\circ\text{C}$  for 3 h, was 3%. Fresh fly ash has been washed in distilled water and removed the carbon that creamed up during washing. It is then dried at 100  $^\circ\text{C}$  for 48 h to remove water. Dried fly ash has been sieved using ASTM meshes ranging in size from 72 to 350. Fly ash fractions after passing through 200 mesh has been taken for ball milling since it gave 45% by weight of the total fly ash taken for sieving, the other size ranges providing less quantity.

### High Energy Pulverization of Fly Ash

The reduction in particle size of fly ash from micron level to the nano level was carried out using a high-energy planetary ball mill (Pulverisette, Fritsch, Germany). The total duration of milling was 60 hours. The following milling conditions were maintained: loading of the ball mill with 10:1 ratio of balls to fly ash and milling chamber and balls were of tungsten carbide, the ball diameter was 10 mm. Toluene was used as the medium with an anionic surface active agent to avoid agglomerations; rotation speed of the planet carrier was 300  $\text{rev min}^{-1}$ .

### Particle Size, Surface Area and Surface Energy Measurements

Particle size of ball milled fly ash at different time of milling was determined using dynamic light scattering technique in a Brookhaven particle size analyzer. Specific surface area of the ground fly ash was found out by using BET method. The samples were degassed at 350  $^\circ\text{C}$  before testing. The surface energy of the samples was calculated by measuring contact angle. The powder contact angles were found out using Dynamic Contact angle Tester (DCAT) from Dataphysics, UK.

The surface free energy of a particle gives an estimate of its surface reactivity. Fowkes [12] proposed a relation based on the surface energy of the material in its pure phase ( $\gamma_a$ ), which is a sum of the contribution from the dispersion ( $\gamma_a^d$ ) and the polar ( $\gamma_a^p$ ) components and may be represented as;

$$\gamma_a = \gamma_a^d + \gamma_a^p \quad (1)$$

The dispersion component mainly consists of London and dispersive interactions, induction (Debye) and orientation interactions, while the polar interactions mainly due to the hydrogen bonding [13]. These components can be derived from Young's equation as given below

$$\cos\theta + 1 = \frac{2(\gamma_s^d\gamma_l^d)^{1/2}}{\gamma_l} + \frac{2(\gamma_s^p\gamma_l^p)^{1/2}}{\gamma_l} \quad (2)$$

Subscripts *s* and *l* represent solid and liquid states respectively and  $\theta$  represents the contact angle of the liquid and the material surface. The work of adhesion could also be obtained from the equilibrium contact angle  $\theta$  as per the equation;

$$W_a = \gamma_l(1 + \cos\theta) \quad (3)$$

### X-Ray Diffraction Studies

The X-ray diffraction measurements were carried out with the help of a Goniometer model PW1710 using CuK $\alpha$  radiation ( $K\alpha = 1.54056$  Å) at an accelerating voltage of 40 kV and a current of 20 mA. The samples were scanned in the range from 10 to 90 degrees 2-theta.

### Infrared Spectroscopy Studies

A Fourier Transform Infrared Spectroscopy (Perkin Elmer FTIR) was employed for examining the functional groups on the fresh as well as ball milled fly ash. The powder samples were ground with spectroscopic grade KBr and made into pellets according to the specified sample preparation procedure.

### Morphology Studies

The size and dimensions of fresh as well as ball milled fly ash were examined by means of electronic microscopy. Scanning Electron Microscope (JEOL JSM 850) and Transmission Electron Microscope (Philips CM 12) were used for the particle surface as well as surface texture analysis.

## Results and Discussion

Results of the Energy Dispersed X-ray analysis (EDX) of the fresh fly ash are shown in Table 1

As per ASTM C 618 [14] fly ash has been classified into two categories, Class F and Class C. The fly ash that contains more than 70% oxides of silicon, aluminium and iron of the total composition with Fe<sub>2</sub>O<sub>3</sub> content higher

**Table 1** Composition of the fresh fly ash (Class F)

% Elemental composition		% Oxide composition	
Component	Content (%)	Component	Content (%)
Aluminium	33.71	Al <sub>2</sub> O <sub>3</sub>	32.16
Silicon	54.84	SiO <sub>2</sub>	59.23
Calcium	1.41	CaO	0.99
Iron	6.97	Fe <sub>2</sub> O <sub>3</sub>	5.03
Titanium	3.07	TiO <sub>2</sub>	2.59

than CaO is termed as Class F type. According to the calculations carried out based on EDX analysis the overall composition of fly ash obtained for this study consists of major proportion of SiO<sub>2</sub>, Al<sub>2</sub>O<sub>3</sub> and Fe<sub>2</sub>O<sub>3</sub>, which seems up to 97.42%. More over the percentage of calcium oxide, which is 0.99%, is less than that of iron which is 5.03%. This observation reveals that the procured fly ash is Class F type.

Variation in composition of metallic oxides with milling time, as determined from EDX analysis are shown in Table 2. The percentage of alumina reduces marginally and the percentage of silica increases marginally as milling for 20 h, there after it remains unaffected with milling time. TiO<sub>2</sub> percent decreases and those of CaO and Fe<sub>2</sub>O<sub>3</sub> marginally increased with long hours of milling.

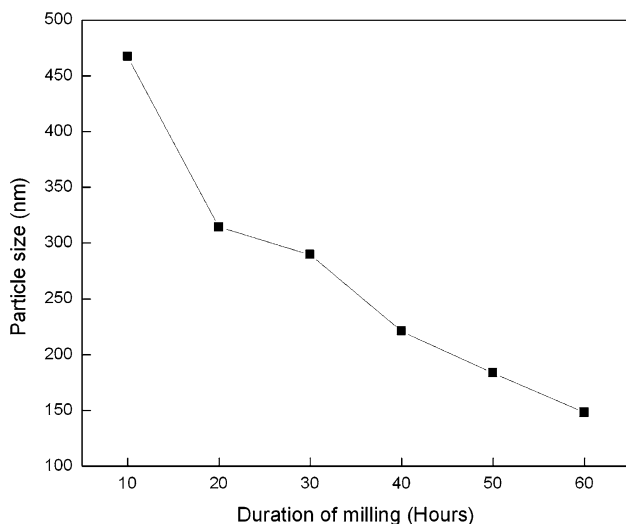
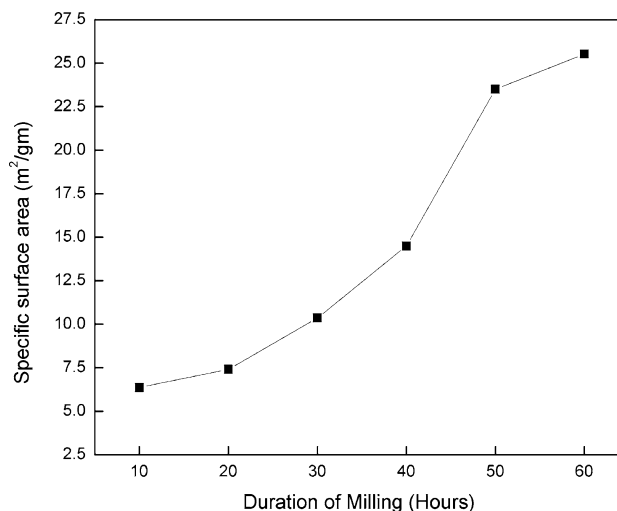
### Particle Size, Surface Area and Surface Energy Measurements of Fly Ash

The variation in particle size and specific surface area of fly ash with milling time is depicted in the Figs. 1 and 2, respectively. The average particle size of the fly ash procured was 60  $\mu$ m. Ball milling of fresh fly ash up to 60 h reduced its size by a magnitude of 405 times to 148 nm. The specific surface area has increased from 0.249 m<sup>2</sup>/gm for fresh fly ash to 25.53 m<sup>2</sup>/gm for fly ash ball milled up to 60 h. The increase in surface area has been found to be more than 100 times in magnitude.

Table 3 displays the values of surface free energy and work of adhesion of fresh as well as ball milled fly ash in water and formamide. These parameters have been extensively used to understand the surface characteristics of the materials [15]. The total surface free energy has increased from 19.223 mJ/m<sup>2</sup> for fresh fly ash, to 56.954 mJ/m<sup>2</sup> for ball milled fly ash up to 60 h. Analyzing the components, the polar component found to decrease from 10.85 mJ/m<sup>2</sup> to 0.8724 mJ/m<sup>2</sup> and the dispersive component increased from 8.373 mJ/m<sup>2</sup> to 56.082 mJ/m<sup>2</sup>. The increase in the dispersive component can be attributed to the surface roughness after ball milling which in turn favors Vander Waal's interactions. The effective exposure of more elements to the surface by ball milling can affect its polar

**Table 2** Variation of oxide composition with milling hours

Milling hours	Al <sub>2</sub> O <sub>3</sub> (%)	SiO <sub>2</sub> (%)	CaO (%)	TiO <sub>2</sub> (%)	Fe <sub>2</sub> O <sub>3</sub> (%)
0	32.16	59.23	0.99	2.59	5.03
20	29.13	62.63	1.31	2.54	4.39
40	27.35	63.59	1.28	2.13	5.65
50	28.55	63.14	0.83	1.85	5.63
60	27.8	62.82	1.32	1.99	6.06

**Fig. 1** Variation in Particle size of fly ash with milling time (in hours)**Fig. 2** Variation of Specific surface area of fly ash with milling time (in hours)**Table 3** Surface energy and work of adhesion of fresh as well as ball milled fly ash

Fly ash sample	Surface energy (mJ/m <sup>2</sup> )		Work of adhesion in water (mJ/m <sup>2</sup> )	Work of adhesion in formamide (mJ/m <sup>2</sup> )
	Polar	dispersive		
Fresh fly ash	10.85	8.373	74.045	64.86
Ball milled for 40 hours	9.705	13.188	78.398	72.595
Ball milled for 60 hours	0.8724	56.082	83.27	107.214

nature. The work of adhesion in both water and formamide are found to increase with duration of ball milling. The increased wettability of the surface is expected to promote its compatibility with the polymer matrices when it is used as reinforcing nanostructured filler.

#### X-Ray Diffraction Studies

The changes in the crystalline phases in the fly ash after ball milling have been monitored with the help of wide angle X-Ray Diffraction studies. The X-Ray diffractograms of the fresh as well as ball milled fly ash are given in the Fig. 3. The magnified view of the major peak corresponding to Quartz at 26.58° 2θ (d spacing = 3.3508 Å) is given in Fig. 4. The average crystallite size was determined from the full width at half maximum (FWHM) of the X-ray diffraction peak using Scherrer's equation [16].

$$D = \frac{K\lambda}{B \cos \theta} \quad (4)$$

where D is the particle diameter, λ is the X-Ray wavelength, B is the FWHM of the diffraction peak, θ is the diffraction angle and K is the Scherrer's constant of the order of unity for usual crystals.

Although fly ash exhibits lower degree of crystallinity, but it shows a number of crystalline peaks in the diffractogram. Mullite (Alumino silicate) and quartz (Silica) peaks are significant. Mullite shows strong peaks at 16.402°, 25.999°, 26.22° and 40.821° 2θ values (d spacing of 5.3998, 3.4243, 3.3959 and 2.2087 Å). The quartz exhibits strong peaks at of 20.763° and 26.579° 2θ values (d spacing of 4.2745 and 3.3508 Å). Iron oxide phase shows a peak at 34.856° 2θ value (d spacing of 1.82 Å). An amorphous hump is observed in the diffraction pattern

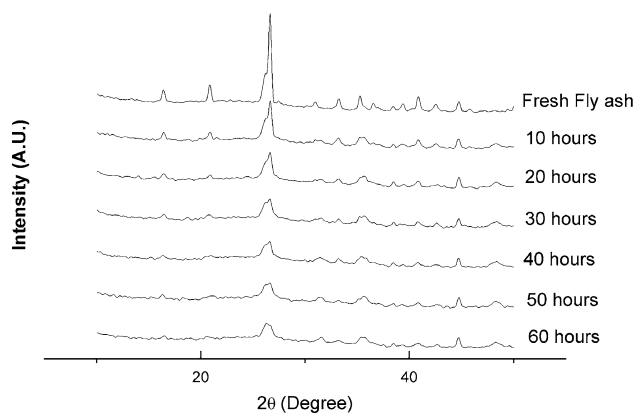


**Fig. 3** X-Ray diffraction patterns of fresh as well as ball milled fly ash at different times

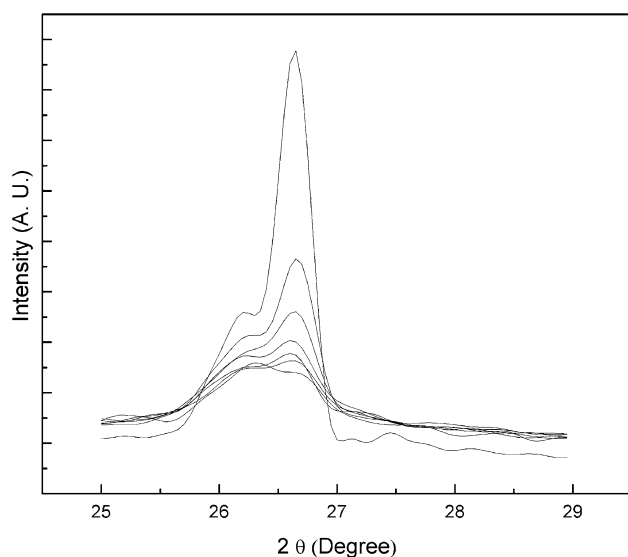


**Fig. 4** Variation in the quartz peak ( $2\theta = 26.58^\circ$ ) height and width with milling times

between approximately  $14^\circ 2\theta$  to  $35^\circ 2\theta$  may be due to the presence of amorphous glassy materials [17].

Figure 5 displays the variation in crystallite size with the time of high energy ball milling. Three major crystalline domains in the fly ash, i.e. quartz, mullite and iron oxide phases were evaluated with the duration of milling. A steady decrease in the crystallite size is observed and the quartz phase suffers the most. The same effect can be seen in the variation of peak height with milling time which is shown in Fig. 6. The high energy milling decreases the crystallinity of the fly ash, thus increasing the amorphous domains in it [18]. The decrease in crystallinity with ball milling hours is depicted in the Fig. 7. This change is beneficial for the applications such as particulate nano filler in polymeric matrices. The enhanced amorphous content is very encouraging as it may lead to better compatibility with various polymeric matrices.

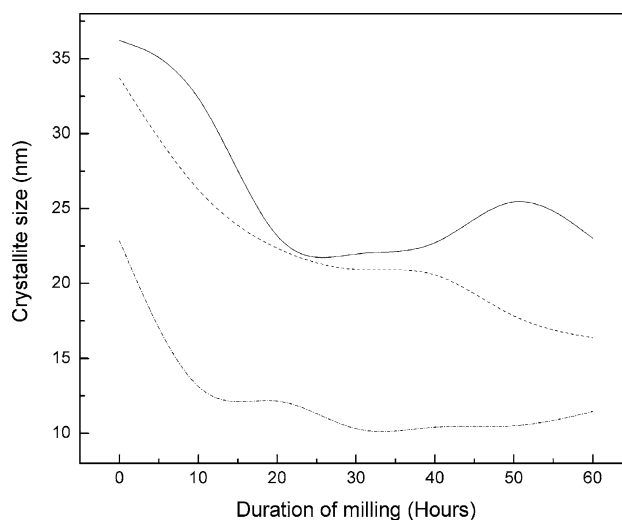


**Fig. 5** Variation in crystallite size with milling time. (—) indicates quartz peak at  $2\theta = 20.86^\circ$ , (- - -) indicates mullite peak at  $2\theta = 40.858$  and (· · · ·) indicates iron oxide peak at  $35.29^\circ$ .

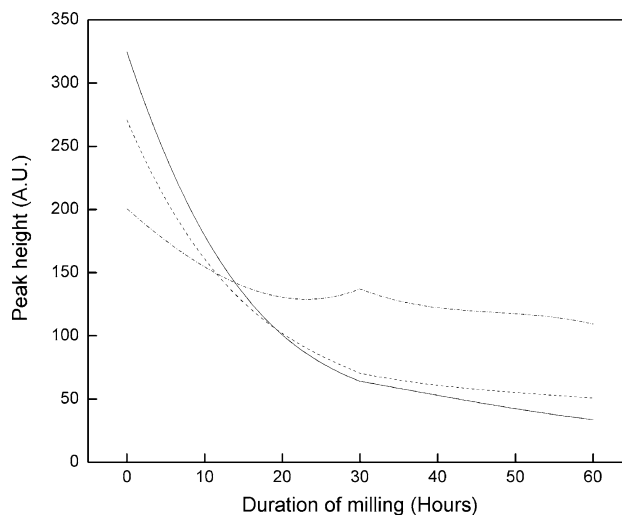


**Fig. 6** Variation in peak height with milling time. (—) indicates quartz peak at  $2\theta = 20.86^\circ$ , (- - -) indicates mullite peak at  $2\theta = 40.858$  and (· · · ·) indicates iron oxide peak at  $35.29^\circ$

#### Infrared Spectroscopy Studies

Figure 8 shows the FTIR spectra of fresh as well as ball milled fly ash. The peak at  $1090\text{ cm}^{-1}$  corresponds to the Si–O–Si stretching vibration [19]. The crystalline quartz ( $\text{SiO}_2$ ) domains are expected to be broken down during ball milling. This has been evidenced from the decreased peak intensity with increasing milling time in the FTIR spectrum. The peak at  $3448\text{ cm}^{-1}$  which was insignificant in the fresh fly ash, has become conspicuous in case of ball milled fly ash. This has been attributed to the presence of silanol (Si–OH) functional group in the fly ash. The peak intensity at this wave number is found to increase with increasing

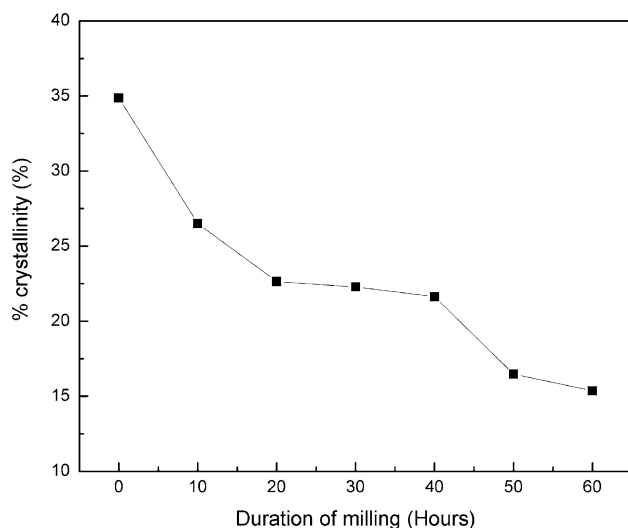


**Fig. 7** Variation in % crystallinity with milling time

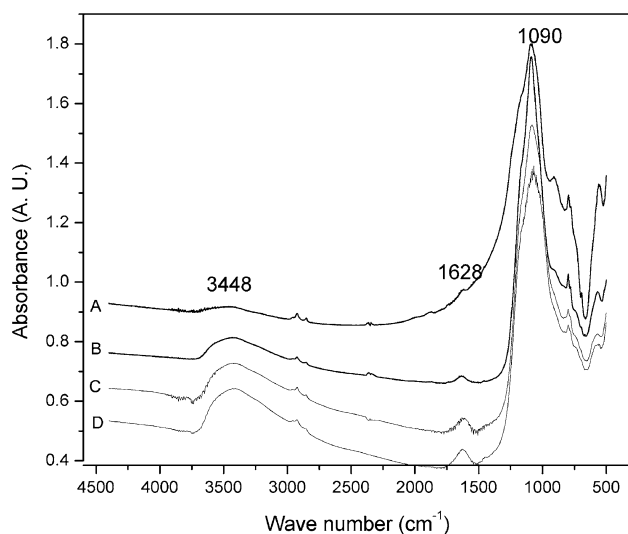


**Fig. 8** FTIR spectrum of fresh and ball milled fly ash at varying time, (A) Fresh Fly ash, (B) Ball milled for 20 h, (C) Ball milled for 40 h and (D) Ball milled for 60 h

milling time is an evidence for the breaking down of the quartz structure and formation of Si–OH groups. The surface properties of the fly ash changes considerably with ball milling and its duration. This has been supported by the surface free energy data. The dispersion forces increase so as the surface reactivity as the OH groups at the surface are increased.

#### Morphological Studies

The size, shape and surface texture of the fresh as well as nano-structured fly ash were studied using Secondary Electron Imaging (SEI) mode of Scanning Electron Microscopy (SEM). Figure 9(A and B) shows the SEM

images of fresh fly ash. The fresh fly ash particles are mostly spherical in shape having an average diameter of more than 10  $\mu\text{m}$ . The morphology of fly ash particle is controlled by combustion temperature and cooling rate. During combustion, inorganic materials in coal become fluid-like at high temperature and then get solidified. In the pulverized coal fired boiler, the furnace operating temperature often exceeds 1400  $^{\circ}\text{C}$ . At these high temperatures, the minerals present in the coal may oxidize, decompose, fuse, disintegrate or agglomerate giving different morphologies to the generated fly ash. Along with the solid spheres, irregular shaped particles of un-burnt carbon can be seen which are large in size. Also agglomerated spheres and irregularly shaped amorphous particles can be detected which may be due to the inter-particle fusion during rapid cooling. Figure 9(C–H) shows the SEM images of nano-structured fly ash after different times of ball milling. Figure 9 (C and D) corresponds to the photomicrographs of nano-structured fly ash after 20 h of ball milling. The spherical structure of fresh fly ash has been destroyed and the average particle size is reduced. The extent of structure break down is more as the duration of ball milling increases and the particles become finer. Figure 9 (G and H) shows the ball milled fly ash after 60 h of milling. It is observed that the SEM analysis is not capable of detecting a single particle even at higher magnifications.

Hence Transmission Electron Microscopy (TEM) was used as an efficient tool to study the microstructure, shape and surface texture of a single fly ash particle. Figure 10(A and B) shows the TEM images of fly ash single particles ball milled for 60 h at very high magnifications of 30,000 and 50,000 times, respectively. Both the images show that the size of the single fly ash particle is in the nanometer range after 60 h of ball milling. Thus nano-structured materials are expected to be present in the ball milled fly ash. Also the surface of the fly ash has changed from glassy smooth to irregular and rough. The outer glassy finish of the fresh fly ash may have been eroded during ball milling and the inner crystalline core may have been exposed after ball milling for 60 h. The increased surface roughness supports the higher surface energy of ball milled fly ash which was discussed earlier in this paper.

#### Conclusions

The size reduction of fly ash from micrometer level to nano levels has been achieved by high energy ball milling. The average particle size has been reduced from 60  $\mu\text{m}$  to 148 nm, a reduction of nearly 405 times in magnitude, by this process. The surface area shows a tremendous increase by around 102 times in magnitude. The total surface free energy has increased by 300% after ball milling for 60 h.

**Fig. 9** The Scanning Electron microscope photomicrographs of fresh and modified fly ash. (A and B) SEM of fresh fly ash at 1,000 and 2,500 times magnification, (C and D) SEM of ball milled fly ash for 20 h at 1,000 and 3,000 times magnification, (E and F) SEM of ball milled fly ash for 40 h at 1,000 and 3,000 times magnification, (G and H) SEM of ball milled fly ash for 60 h at 1,000 and 3,000 times magnification

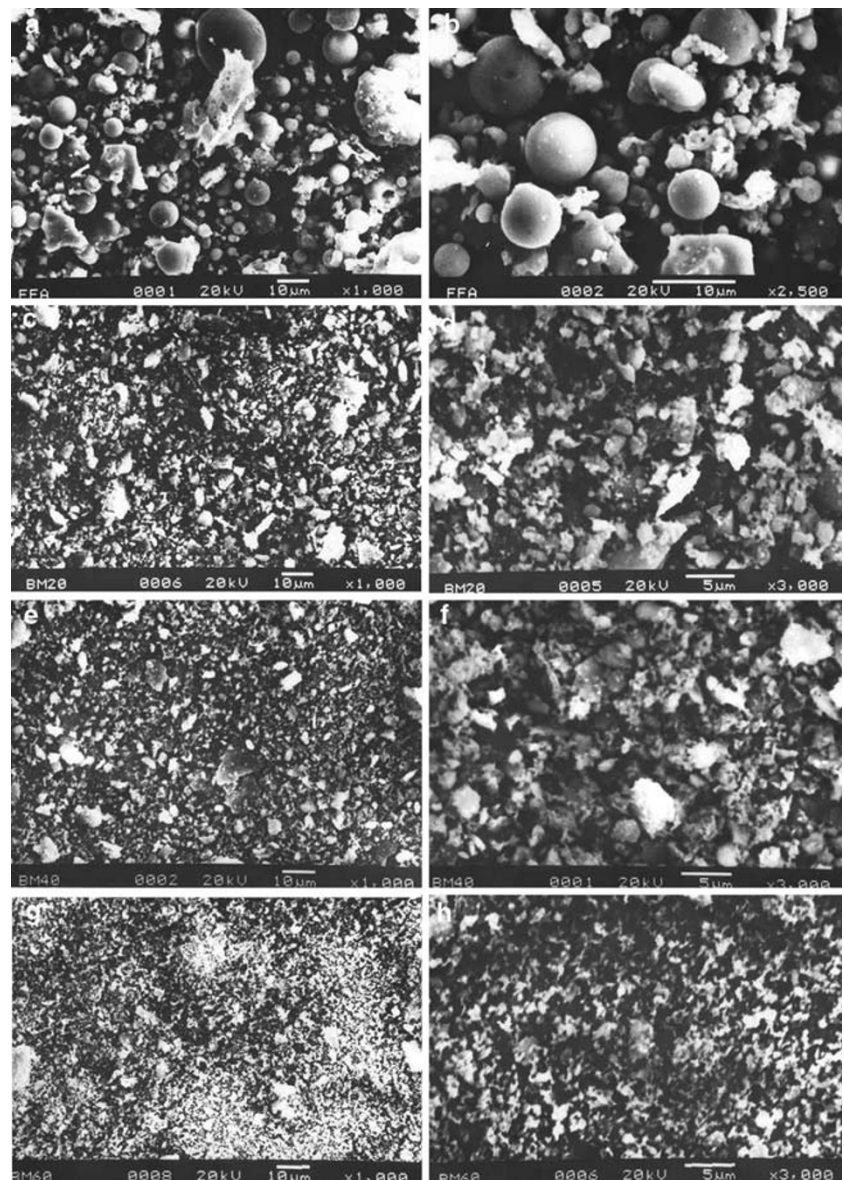
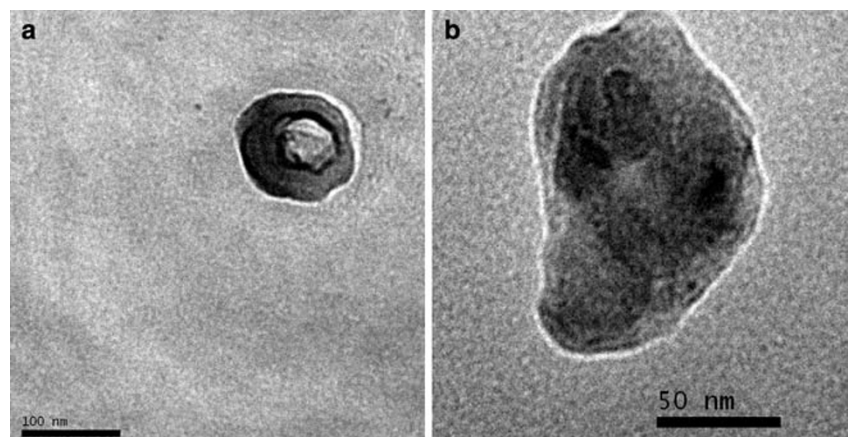


**Fig. 10** (A and B) TEM images of fly ash ball milled for 60 h



The characteristic –OH stretching vibration peak intensity increases by ball milling. The fly ash becomes more amorphous and the crystallite size reduces drastically. The shape and surface texture of the fly ash has been changed by ball milling which is evident from TEM and SEM studies. The nanostructured fly ash may be effectively used as reinforcing filler in polymer matrices.

**Acknowledgements** The authors would like to thank Ms. Sasmitha Mohapatra, Department of Chemistry, Indian Institute of Technology, Kharagpur for particle size analyses and IRMRA, Thane, India for surface area measurements.

## References

1. B. Bhushan, in *Springer Handbook of Nanotechnology* (Springer-Verlag, Germany, 2004)
2. M.G. Lines, *J. Alloys Compd.*, doi:10.1016/j.jallcom.2006.02.082 (2007)
3. A.S. Edelstein, in *Encyclopedia of Materials: Science and Technology*, ed. by K.H.J. Buschow, R.W. Cahn, M.C. Flemings, B. Ilschner, E.J. Kramer, S. Mahajan, P. Veyssiere (Elsevier Science and Technology, 2006) p. 5916
4. C. C. Koch, *Rev. Adv. Mater. Sci.* **5**, 91 (2003)
5. G. Chow, L.K. Kurihara, in *Nanostructured materials: Science and Technology*, ed. by C.C. Koch (William Andrew Inc. N.Y., 2002)
6. H.J. Fecht, *Nano Struct. Mater.* **6**, 33 (1995)
7. S. Doppiu, V. Langlais, J. Sort, S. Suriñach, M.D. Baro, Y. Zhang, G. Hadjipanayis, J. Nogués, *Chem. Mater.* **16**, 5664 (2004)
8. R. Giere, L.E. Carleton, G.R. Lumpkin, *Am. Mineral.* **88**, 1853 (2003)
9. S.C. White, E.D. Case, *J. Mater. Sci.*, **25**, 5215 (1990)
10. V. Kumar, K. Abraham Zacharia, P. Sharma *Fly Ash Utilisation: Indian Scenario & Case Studies*. <http://www.tifac.org.in/news/flyindia.htm> as on 15 April 2007
11. Ash Utilization, National Thermal Power Corporation (NTPC), India <http://www.ntpc.co.in/infocus/ashutilisation.shtml> as on 14 April 2007
12. F.M. Fowkes, in *Treatise on adhesion and adhesives*, vol 1, ed. by R.L. Patrick (Marcel Dekker Inc., N.Y., 1967)
13. E. Chibowski, L. Holysz, *Langmuir* **8**, 710 (1992)
14. ASTM C 618, 'Standard Specification for Coal fly ash and Raw or Calcined Pozzolan for use as a mineral admixture in concrete', ASTM International, West Conshohocken, Pa., 4 (1997).
15. A. K. Bhowmick, J. Konar, S. Kole, S. Naryan, *J. Appl. Pol. Sci.* **57**, 631 (1995)
16. A.L. Patterson, *Phys. Rev.* **56**, 978 (1939)
17. P. Jason Willians, J.J. Biernacki, C.J. Rawn, L. Walker, J. Bai, *ACI Mater. J.*, **102**(5), 330 (2005)
18. L. L. Shaw, R. Ren, Z. Ban, Z. Yang, *Ceramic nanomaterials and nanotechnology*, vol. 137 (American Ceramic Society, Ohio, 2003)
19. S. Thongsang, N. Sombatsompop, *Polym. Compos.* **27**, 30 (2006)